Journal of Power Sources 241 (2013) 560–566

Contents lists available at SciVerse ScienceDirect

Journal of Power Sources

journal homepage: www.elsevier.com/locate/jpowsour

Empirical analysis of contributing factors to heating in lithium-ion cells: Anode entropy versus internal resistance

Rengaswamy Srinivasan*, Bliss G. Carkhuff

Applied Physics Laboratory, The Johns Hopkins University, Laurel, MD 20723-6099, USA

HIGHLIGHTS

- Describes role of anode entropy in heat generated during charging of Li-ion cells.
- Identifies transition to overcharge by sensing transition in anode temperature.
- Provides a path to fast-charge Li-ion cells without the fear of venting.
- Describes a procedure to fully charge Li-ion cells using constant current-only step.
- Demonstrates that CC-only procedure does not accelerate capacity fading.

ARTICLE INFO

Article history:
Received 31 January 2013
Received in revised form
18 April 2013
Accepted 21 April 2013
Available online 7 May 2013

Keywords:
Anode entropy
Entropy-generated heating
Anode temperature transition
Overcharge protection
Fast charging

ABSTRACT

Charging a battery beyond its maximum capacity can lead both to cell overheating and to the venting of gasses. A fundamental understanding of cell heating could lead to the development of real-time sensors that anticipate and avert catastrophic battery failure. Joule heating (also called ohmic or resistive heating) from cell internal resistance (R_{int}) dominates the overall thermal energy (ΔQ) generated during charging. Contrary to prior hypotheses, though, Joule heating does not appear to contribute to venting observed during overcharging. In this manuscript, we examine an alternate hypothesis, that heat released by the entropy change in the anode (ΔS_{anode}) and the concomitant increase in the anode temperature (T_{anode}) triggers the venting. Using our recently developed non-invasive battery internal temperature (BIT) sensor to monitor T_{anode}, we separated the contributions of ΔS_{anode}, R_{int} and the anode resistance (R_{anode}) to ΔQ. These quantities were tracked during constant current charging of a 18650 Lithium-ion cell, from zero state of charge (SoC) to overcharge. The resulting analysis suggests that anode entropy change is more important than resistive heating resulting from R_{anode} to the overall thermal energy. Anode entropy measurements, enabled by the BIT sensor, might serve as an alternative or adjunct method for anticipating and avoiding cell venting events.

1. Introduction

The process of charging a lithium-ion cell generates heat. A sufficient rise in cell temperature causes the contents of the cell to decompose, releasing fumes in a dangerous process called venting. A basic scheme for detecting cell venting is based on measuring the cell temperature at its external surface (T_{surf}), followed by inferring the cell's interior temperature through thermal modeling [1–3]. The cell's thermal inertia causes this approach to incur significant delay in transferring heat from inside to the cell's external surface. The time delay between start of a thermal process inside the cell and the transfer of heat to surface is on the order of tens of seconds [4]. This significant delay renders techniques for avoiding venting that depend on T_{surf} monitoring ineffective. Invasive techniques that involve placing thermal sensors inside the cell have been attempted as alternatives to surface mounted sensors [5,6]. Invasive sensors have the potential to alleviate partially the time delay issue. However, using these sensors poses other problems, including instability of sensor readings in the aggressive environment of the cell's interior, and including additional sealants for the sensor's port. A non-invasive sensor that senses the internal temperature instantly while the cell is under charge and discharge is most desirable. More importantly, a non-invasive sensor that facilitates the fundamental understanding of the heat generating process would also allow the efficient prediction of cell venting, thereby enabling safe and rapid cell charging.

* Corresponding author. Tel.: +1 443 778 6378; fax: +1 443 778 5937.
E-mail addresses: Rengaswamy.srinivasan@jhuapl.edu, srinir@comcast.net (R. Srinivasan).

0378-7753/$ – see front matter © 2013 Elsevier B.V. All rights reserved.
http://dx.doi.org/10.1016/j.jpowsour.2013.04.108

There are two main reasons for heat generation during charging: 1. Internal resistance (R_{int}); and 2. Change in anode entropy (ΔS_{anode}) [7]. In the past, it has been generally assumed that R_{int} is the primary contributor to cell heating and venting, especially at high rates of charging and discharging [8,9]. Of course, every cell has an internal resistance, and it does dissipate power (P_{resist}) from the current generated during charging (I_{charge}). Inside the cell, the current is carried between the cathode and the anode by cations (lithium ion) and anions (usually phosphate ion) in the electrolyte, and the ionic resistance contributes partially to R_{int}. Additional contributions to R_{int} come from charge transfer resistances, R_{anode} and $R_{cathode}$, associated, respectively, with the flow of the charge species (Li^+ ion) across the anode and the cathode. Thus, $R_{int} = R_{anode} + R_{cathode} + R_{elec}$, where R_{elec} is the resistance due to the electrolyte. The governing equation for thermal power generation due to R_{int} is $P_{resist} = I^2_{charge}\, R_{int}$.

Change in anode entropy during charging is a different process from cell internal resistance. Most lithium-ion (Li-ion) cells use carbon anode. As the state of charge (SoC) increases from 0% to 100%, the percentage of sites in the anode that are occupied by lithium increases from 50% to 100% causing a decrease in the entropy of the carbon anode [10–12]. The second law of thermodynamics relates this change in entropy to heat: $\Delta Q_{anode\ entropy} = T_{anode}\Delta S_{anode}$. To date, accurate in situ measurements of T_{anode} have been difficult to achieve because the anode is contained within the cell. As a result, it has been difficult to continuously estimate the specific contribution of anode entropy to cell heating. A first-order estimation of heat generated by ΔS_{anode}, R_{int} and R_{anode} helps identify their relative contributions to ΔQ.

Consider, for example, 18650 cells with 2.6-Ah capacity that is commonly used to power laptop computers. Such cells are generally charged at C/2 rate (1.3 A rate; C is the Ah capacity). Table 1 below summarizes the estimated values of thermal energy, ΔQ associated with entropy change in the anode and resistive heating in the anode during C/2 charging and 2C rate charging of the 18650 Li-ion cell under ambient conditions from close to complete discharge (SoC <1%) to near full charge (SoC >99%).

The data in Table 1 was arrived through the following assumptions. Charging the cell to a capacity of 2.6 Ah using a 1.3 A current source requires 6923 s and 0.0932 mol of lithium by Faraday's law. Assuming $\Delta S = -8$ J mol^{-1} of Li/K for the carbon anode [10,11], the entropy change for 0.0932 mol of lithium is 0.7456 J K^{-1}. Assuming for simplicity that $T_{anode} = 300$ K over the course of charging, a total of 224 J in thermal energy is dissipated at a rate of 32.3 mW. In comparison, Joule heating by the anode resistance ($I^2_{charge}\, R_{anode}$) dissipated 10 mW: Note from Fig. 1 that R_{anode} is about 6-mΩ, and a 1.3-A current passing through a 6-mΩ will generate 10 mW, and the course of charging from 0 to 2.5-Ah for 6923 s, Joule heating alone would generate 70.2 J of energy. R_{int} was assumed to be 60-mΩ (based on the data in Fig. 1b) in arriving at the thermal energy and thermal power associated with it. Two additional issues not highlighted in the table includes: i.) When SoC → 100%, ΔS changes from −8 J mol^{-1} K^{-1} to −18 J mol^{-1} K^{-1} [10], changing the rate of heating due to entropy changes from 32.4 mW to 72.7 mW; and ii.) During charging, R_{anode} decreases with an increase in SoC, as can be seen from the data in Fig. 1a, resulting in a decreasing Joule heating even as the cell is being charged up to and beyond its capacity. Estimates shown in the last two columns of Table 1 correspond to 2C charging rate (5-A rate), based on the same set of assumptions as the C/2 rate, except that T_{int} is 320 K. Note that even at 2C rate, the rate of heating due to anode entropy dominates over the anode's Joule heating.

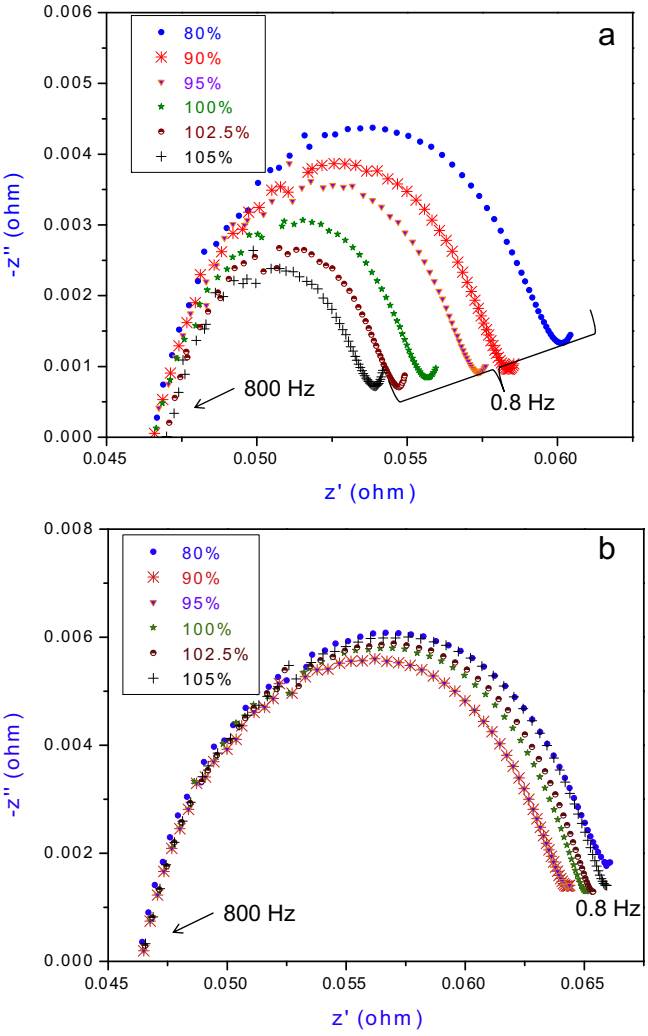

Fig. 1. Impedance of a 2.6-Ah SDI 26F 18650 Li-ion rechargeable cell at 23.5 °C T_{env}, at various levels of SoC and T_{surf} as indicated: (a) while the cell was under charge, the charging current caused the cell's current capacity and its surface temperature to increase; and (b) after stopping the flow of the charging current and equilibrating T_{surf} with T_{env}. Each point in the graphs represents impedance data at one of 61 separate frequencies between 0.8 and 800 Hz; the end frequencies are shown in the figure.

These estimates indicate that the major source of heating experienced at the anode during charging is the entropy change at the anode. We have gathered experimental evidence to corroborate this hypothesis using a 2.6-Ah 18650 Li-ion cell. These data, described in the next section, validate the hypothesis that ΔS_{anode} is the major contributor to cell venting during overcharge. Recently, we developed a battery internal temperature (BIT) sensor to non-invasively

Table1
Estimates of individual contributions by ΔS_{anode}, R_{int} and R_{anode} to heat energy, ΔQ generated during charging of a 2.6-Ah 18650 Li-ion cell.

Parameter contributing to heat generation	Thermal energy generated during C/2 charging (J)	Thermal power generated during C/2 charging (mW)	Thermal energy generated during 2C charging (J)	Thermal power generated during 2C charging (mW)
ΔS_{anode}	224	32.3	238.6	149.1
R_{anode}	70.2	10.1	30	18.8
$R_{int} = R_{anode} + R_{cathode} + R_{elec}$	702	101.4	300	187.5

measure T_{anode} [13–15]. In the present work, we exploit this technological advance to measure T_{anode} in real-time, during the charging process. We estimate ΔS_{anode} as an empirically-derived function of state of charge (SoC) based on the literature. These values are combined to generate an estimate of $\Delta Q_{anode\ entropy}$, the contribution of anode entropy to overall cell heating. Because empirically-derived estimates of ΔS_{anode} are known to underestimate anode entropy during overcharging, the overall estimate of $\Delta Q_{anode\ entropy}$ is an approximate lower bound. In the following experiments, we show that even this approximate lower bound contribution to the overall cell heating by entropy heating is more than three times the contribution by the resistive heating $I^2_{charge}\,R_{anode}$.

2. Experimental

Commercial 18650 cells, model SDI 26F, with mixed metal oxide (NCM/LCO) cathode and carbon anode were used as test candidates. Cells of this capacity and model are most commonly used in most laptop computers and other electronic gadgets – they have a ubiquitous presence in public and private spaces. The nameplate capacity of each cell was 2.6-Ah; its nominal capacity was lower (~2.5-Ah), as is the case with almost all Li-ion cells (The 2.6-Ah nameplate capacity can only be obtained through an infinitesimally slow charging process; the lower nominal capacity represents real-world values obtained when the cell is charged over a period of 3–6 h.). All cells were obtained fresh, and were subject to conditioning through two full charge–discharge cycles at room temperature (23.5 °C) at C/2 rate; the lower cell voltage cut-off during discharge was 2.7 V, and CC–CV charging included constant current charging to 4.2 V, and holding the voltage at 4.2 V while allowing the cell current to drop to C/20 (0.13-A). Following conditioning, we charged the cell to full capacity (2.5-Ah), discharged it by 0.13-Ah, and allowed it to rest at room temperature for 24 h before further testing.

All tests were conducted at room temperature under ambient conditions. The cell surface was not insulated, and not subjected to forced cooling. At the start of each test, the cell was at 95% nameplate capacity. Before further testing, the environmental temperature (T_{env}), T_{surf} and T_{anode} were measured and validated for consistency; the 24-h resting after the conditioning was necessary for consistency across the three temperatures. Next, immediately before subjecting the cells to charging and overcharging, the cells were fully discharged to 2.7 V cut-off. Then, the cells were charged through the constant current-only charging (CC-only) step until the cell's chemical constituents started leaking out, presumably due to the opening of the pressure disc inside the cell; the amplitudes of the charging current were C/2, C/1.7 or 2C. Some of the cells were also subject to the conventional CC–CV charging without intentional overcharging. During charging, we monitored the internal temperature of the cell using a four-probe, electrical, non-invasive technique that was recently developed at the Johns Hopkins University Applied Physics Laboratory (JHU/APL) [13–15]. Note that the technique is predicated on a non-linear relationship between phase shift (ϕ) and T_{anode}. The cell capacity and size can and does affect the relationship [14]. Therefore for reliable measurement of T_{anode} during the charging of the SDI 26F cell, we first established ϕ vs. T_{anode} relationship using the customary procedure described earlier [13–15]. We also monitored the cell's outer surface temperature (T_{surf}) and the cell voltage (E_{cv}) using conventional tools, a thermocouple and a voltmeter.

3. Results and discussions

Published research reports describe high internal temperatures and high cell voltages as the initiators of gas evolution and cell venting during overcharge, through thermal decomposition of the battery chemicals and electrochemical reduction and oxidation of solvents [16,17]. Although these two effects undeniably have the potential to cause venting, the results below show that they may not be the initiators. Instead, the underlying reason for venting appears to be $\Delta Q_{anode\ entropy}$, the thermal energy generated by entropy change in the anode. Tracking $\Delta Q_{anode\ entropy}$ helps identify the cell transitioning from full charge to overcharge and venting; tracking dT_{anode}/dt helps prevent overcharging and venting. Monitoring T_{anode} also facilitates charging using only constant current (CC) charging without the risk of overcharging, eliminate the need for the time-consuming CV step. By this CC-only method, we can minimize the time for complete charging of the battery.

3.1. Monitoring entropy change in the anode and cell venting through CC-only charging

Figs. 2–4 show T_{anode}, T_{surf} and E_{cv} data during CC-only charging at C/2, C/1.7 and 2C rates. All cells were charged immediately after they were fully discharged (end voltage cut-off: 2.7 V) at a 1.3 A rate. Since the discharge process tends to cool the anode due to positive change in its entropy [12], at the beginning of charging, T_{anode} was less than T_{surf} the ambient temperature, T_{env}; discharging also set the T_{surf} above T_{env}.

The results for the C/2 rate charging shown in Fig. 2 demonstrate that E_{CV} and T_{surf} increased monotonically with charging time, until several seconds after the cell vented. T_{anode} on the other hand, showed a markedly different behavior than E_{CV} and T_{surf}. T_{anode} increased at a steady rate only until the cell charged to near full capacity. When the capacity reached 2.5-Ah, which is a little over 96% of its nameplate capacity (2.6-Ah), and quite close to its nominal capacity (2.492-Ah), T_{anode} increased at a faster rate. The inflection point in the rate of increase of T_{anode} versus time (T_{anode} vs. t) is sharp and clearly perceptible; dT_{anode}/dt changed by a factor of ten from 0.0012 K s^{-1} to >0.012 K s^{-1}. After continued charging at the 1.3-A rate for about 10 min past the inflection in the T_{anode}, the cell vented, when the T_{anode} decreased from its peak value. Observable physical damage to the cell caused by venting was

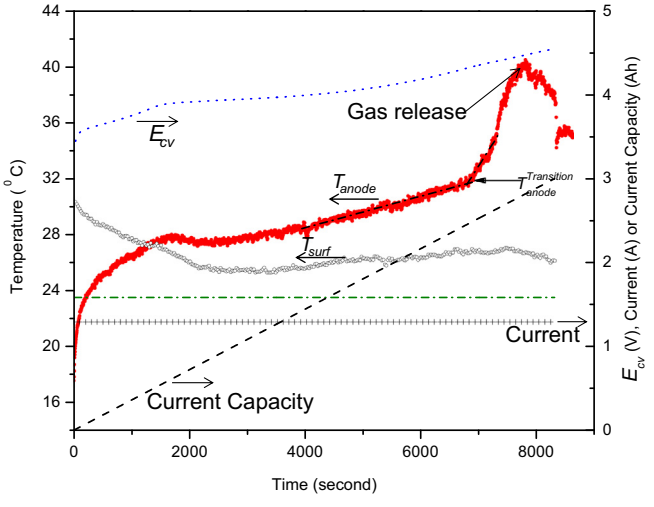

Fig. 2. Anode temperature, T_{anode} (red, solid circles), and T_{surf} (black, open circles) behavior of the SDI 26F 18650 cell in a 23.5 °C environment, while the cell was under C/2 rate charging. Note the transition in dT_{anode}/dt when the current capacity reached 2.5-Ah. Before charging, the cell was discharged at C/2 rate, causing the T_{anode} to drop below T_{env} and T_{surf} to rise above T_{surf}. Also shown in this, and in Figs. 3 and 4, are the drop in T_{anode} when the charging process caused the cell to vent; E_{cv} (blue, dotted line); current capacity (black, dashed line); and current (black, cross). (For interpretation of the references to colour in this figure legend, the reader is referred to the web version of this article.)

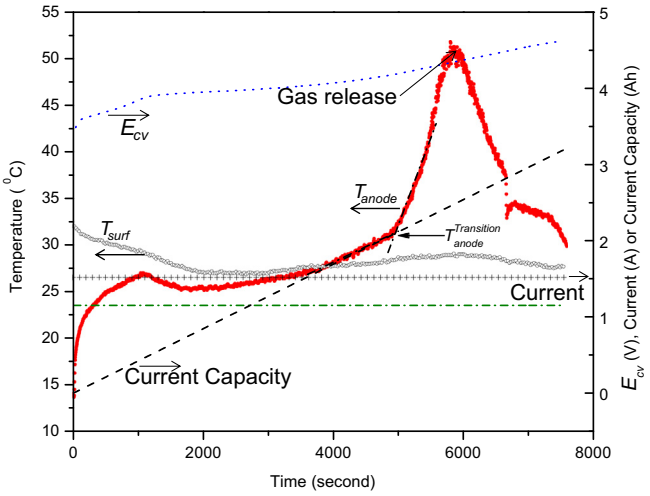

Fig. 3. Anode temperature, T_{anode} (red, solid circles), and T_{surf} (black, open circles) behavior of the SDI 26F 18650 cell in a 23.5 °C environment, while the cell was under C/1.7 rate charging. At the C/1.7 rate, the transition in dT_{anode}/dt occurred when the current capacity reached 2.16-Ah. (For interpretation of the references to colour in this figure legend, the reader is referred to the web version of this article.)

limited to trace amounts of chemicals leaking out through the vent; pressure shutdown feature such as current interrupt device (CID), if there was one inside the cell, did not shutdown the cell.

The sudden change in T_{anode} observed when the capacity reached 2.5-Ah is related to the entropy change in the anode. Charging displaces lithium ions from the electrolyte into the carbon anode, in the process decreasing the entropy of the carbon–lithium composite. Note that in the most commonly accepted model, during charging, the lithium ion that enters the carbon electrode is partially reduced; it intercalates with carbon and occupies the center of the six-member carbon ring created by the sp^2-hybridized graphene plane [18,19]. The total number of six-member rings in the carbon electrode limits the sites that lithium could occupy. Thus, charging sequesters the lithium ions, decreases the entropy of the anode, and increases the T_{anode} until nearly all-available sites in the carbon electrode are taken by lithium. Attempts to push more lithium into the anode result in a sharp change in the entropy (from $-8\,J\,mol^{-1}\,K^{-1}$ to $-18\,J\,mol^{-1}\,K^{-1}$),

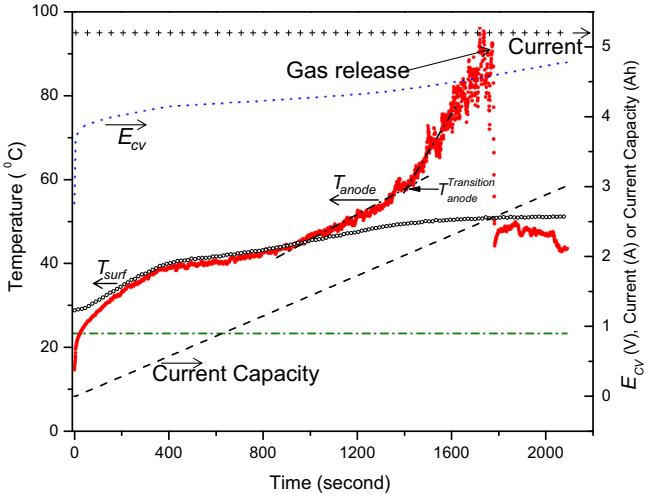

Fig. 4. Anode temperature, T_{anode} (red, solid circles), and T_{surf} (black, open circles) behavior of the SDI 26F 18650 cell in a 23.5 °C environment, while the cell was under 2C rate charging. At the 2C rate, the transition in dT_{anode}/dt occurred when the current capacity reached 2.02-Ah. (For interpretation of the references to colour in this figure legend, the reader is referred to the web version of this article.)

with concomitant sharp increase in T_{anode}; the change in dT_{anode}/dt is more than a factor of ten, and is measurable within seconds. T_{anode} at the point of inflection in the slope was about 304 K, and E_{CV} was 4.29 V. When the cell vented, dT_{anode} had sharply increased to 313.4 K and E_{CV} had gradually crept up to 4.475 V.

Charging the cell at faster rates caused the T_{anode} to rise more quickly, and caused the inflection point in the dT_{anode}/dt slope to occur before reaching the 2.5-Ah capacity as demonstrated in Figs. 3 and 4. Charging at 1.525-A rate, for instance, caused the inflection in the dT_{anode}/dt slope to occur when the cell reached 2.16-Ah capacity or 85% of the 2.6-Ah nameplate capacity.

Charging the cell at 5.2-A (2C) rate provided further insight into the effect of T_{anode} and CV on the limits of reaching full capacity and venting. As seen from the data in Fig. 4, charging at 2C rate also caused T_{anode} to rise faster than at C/2 rate. The inflection in the dT_{anode}/dt slope occurred after 1400 s, at 2.02-Ah (78% of 2.6-Ah capacity), when the T_{anode} was at 332 K, and the CV was at 4.385 V. We observed large fluctuations in T_{anode} during high rates of charging. The cell vented only when T_{anode} was above 368 K, and the CV was 4.467 V. At this point, a charging current of 2.267-Ah had passed through the cell.

We repeated the CC-only charging in the C/2 to 2C rate range (1.3-A to 5.2-A range) in more than ten cells. In each case, the occurrences of the inflection in the dT_{anode}/dt slope when the cell reaches its full SoC are reproducible. Similarly, the incident of gas release with concomitant sudden drop in the T_{anode} upon prolonged overcharging, are also reproducible. Following the gas release, we did not analyze it for chemical composition; such an analysis is beyond the scope of this work. However, GC–MS measurements performed by Kong et al. on the gases associated with three different batteries, namely, Carbon/$LiCoO_2$, Carbon/$LiMn_2O_4$ and Carbon/$LiFePO_4$ indicated that they are a mixture of CO_2, CO, CH_4, C_2H_4, C_2H_6, C_3H_6, C_3H_8, and C_2H_5F [17].

Table 2 provides a summary of experimental entropy-related heating ($\Delta Q_{anode\ entropy} = T_{anode}\Delta S_{anode}$) and Joule heating ($I^2_{charge}\,R_{anode}$) related to charging at different rates, along with the Ah capacity and the T_{anode} values reached at the inflection point in the slope, dT_{anode}/dt. It is striking that at all the three charging rates, when $\Delta Q_{anode\ entropy}$, the energy released by the entropy change in the anode reached about 224 J, the dT_{anode}/dt showed a sudden inflection; the inflection point is independent of the T_{anode} or the T_{surf}. It is also worth noting that for all the charging rates, entropy-generated heat dominates over energy released by Joule heating ($I^2_{charge}\,R_{anode}t$). Finally, neither the inflection point in T_{anode} nor the point where the cell vents is dependent on the T_{anode}, T_{surf} or E_{cv}.

As noted before, the stability of the constituents of the Li-ion cell is limited by its internal temperature and voltage across its terminals. The constituents are stable at temperatures below 373 K; and the solvents are not decomposed at voltages below 4.5 V. Furthermore, during charging, the temperature of the anode increases and that of the cathode decreases; thus the maximum T_{int} cannot exceed that of the anode. The data in Table 1 and in Figs. 2–4 show that during charging at all the rates from C/2 to 2C, the maximum internal temperature does not increase above 373 K, and the cell voltage is below 4.5 V. Nevertheless, all cells charged well above the 224 J of entropy-generated heat showed evidence of venting in the form of trace amounts of chemical leaks. The observations described above demonstrate that venting is not driven by temperature or cell voltage. The sudden increase in dT_{anode}, at any rate of charging indicates that the anode entropy is playing a disruptive role leading to cell venting. The best way to prevent venting appears to be to track the entropy change and to limit it to 224 J for the 18650 cell, or more generally to 2360-J mol^{-1} of lithium insertion into the carbon anode.

Table 2
Experimental values of $\Delta Q_{anode\ entropy}$ and $I^2_{charge}\,R_{anode}t$ at different charging rates, along with the Ah capacity and the T_{anode} values reached at the inflection point in the slope, dT_{anode}/dt.

Charging current (A)	T_{anode} (K) and T_{surf} (K) at dT_{anode}/dt inflection	Capacity (Ah) and E_{cv} (V) at dT_{anode}/dt inflection	Heat released due to $\Delta S_{anode}T_{anode}$ (J)	Heat released due to $I^2_{charge}R_{anode}t$ (J)	T_{anode} (K)/T_{surf} (K) and cell voltage (V) at venting
1.3	304/299.8	2.5/4.290	224.9	70	313.4/300 4.475
1.525	304/301.3	2.16/4.181	219.5	71	323/302.1 4.339
5.2	332/322.5	2.02/4.385	226.1	113.5	368/323.7 4.467

3.2. CC–CV: the conventional approach to charging

The charge and energy capacities obtainable through the CC–CV charging procedure help identify its merits and limitations, and how it contrasts with the less conventional CC-only charging.

Even though CC–CV is the most common and conventional two-step charging procedure, the details within the two steps (CC and CV) vary between applications and users. More importantly, the variations can and do generate differences in the duration of charging and in the charge and energy capacities of the cell. For example, the two extremes of the CC step could involve a small current on the order of C/4 that charges the cell slowly or a large current on the order of C/2 that charges quickly. The C/4 generates less heat at the expense of long charging time than the C/2. The CV step may include protocol to terminate charging when the current drops to C/20 or C/200; the latter adds more capacity to the cell, obviously at the expense of longer charging time. We followed the conventional protocols and designed two extreme CC–CV charging procedures for the SDI 26F 18650 cell.

Procedure 1: Step 1, CC: 1.3-A constant current (C/2), until the cell voltage reached a pre-set high cut-off value of 4.2 V; Step 2, CV: 4.2 V, until the charging current dropped from the initial high value (C/2) to C/20, i.e., 1.3-A to 0.13 A. Through this procedure, the cell capacity reached 2.492-Ah in 2 h and 23 min; in Step 1, the cell reached 2.155-Ah (83% capacity) in 1 h and 40 min.

Procedure 2: Step 1, CC: 0.65-A constant current (C/4), until the cell voltage reached a pre-set high cut-off value of 4.2V; Step 2, CV: 4.2 V, until the charging current dropped from 0.65 A (C/4) to 0.013 A (C/200). Through this procedure, the cell capacity reached 2.55-Ah in 5 h and 24 min; in Step 1, the cell reached 2.335-Ah (90% capacity) in 3 h and 36 min.

Obviously, one could achieve higher than 2.55-Ah capacities at excruciatingly slower rates by changing the CC–CV protocols to much smaller currents. Today, the CC–CV protocols similar to the ones described above are considered the normal path to charging a cell to its full nominal capacity. Generally, these charging protocols are slow. By contrast, CC-only charging procedure at a C/2 rate charged the cell to 2.5-Ah in 1 h 55 min–28-min sooner (20% faster) than Procedure 1 and 3.5 h sooner than Procedure 2. The question is: Are the CC–CV protocols anchored in the principles governing cell safety or are they arbitrary?

The conventional explanations for the CC–CV protocols are that: i.) they safeguard against electrolysis of the solvent by restricting the cell voltage far below the oxidation potential of the solvent; and ii.) they keep the T_{int} low, presumably through diminished Joule heating. These arguments have merits; however, their validity may be exaggerated. Oxidation of the solvents in Li-ion cells actually occurs at a much higher potential than 4.2 V [20], that begs the question: Can the cut-off voltage be higher than 4.2 V? The conventional (CC–CV) procedure appears to set a lower and arbitrary limit on voltage at the expense of extended charging time.

Furthermore, attempts to smaller cut-off current in the CV step adds little value to the cell capacity, as demonstrated above under Procedure 2. Charging to full capacity using the CC-only step would charge the cell in shorter time; however, is deemed risky due to the possibility of raising the E_{cv} to dangerously high values, and heating the anode and causing it to react with the solvent. We demonstrate next that online monitoring of the T_{anode} helps eliminate the risk associated with uncertainty of knowing when to stop charging.

3.3. CC-only charging and cell degradation

Would CC-only charging degrade the cell any faster than the conventional CC–CV charging? Based on one 204-cycle, with the CC-only charging at C/2 rate, followed by 100% depth-of-discharge at C/2 rate to 2.75 V at 23 °C, the cell recorded a <20% capacity fading. During each cycle, the CC-only step charged the cell to 2.5-Ah capacity, and discharged it to 2.75 V; the discharge capacity was about 2.478-Ah over the entire 204 cycles. At the end of the 204th cycle, the cell was subject to 6 additional cycles of conventional CC–CV charging, and CC-only discharging. The CC–CV charging step used 1.3-A current to 4.2 V for the CC part, and 4.2 V holding potential for the CV part until the current dropped to 0.13 A. The CC-only discharging used a 1.3-A constant current down to 2.75 V cell voltage. The charge and discharge capacities between 205 and 211 cycles are shown in Fig. 5; discharges at the 206 and 211 cycles were limited to 1.3-Ah in order to measure the impedance at about the 50% SoC mark, hence their full discharge capacities are not available. The cell charged well above 2.07-Ah and discharge to well above 2.06-Ah, suggesting it retained a >80% of the 2.5-Ah discharge capacity. The <20% capacity fading is no worse than

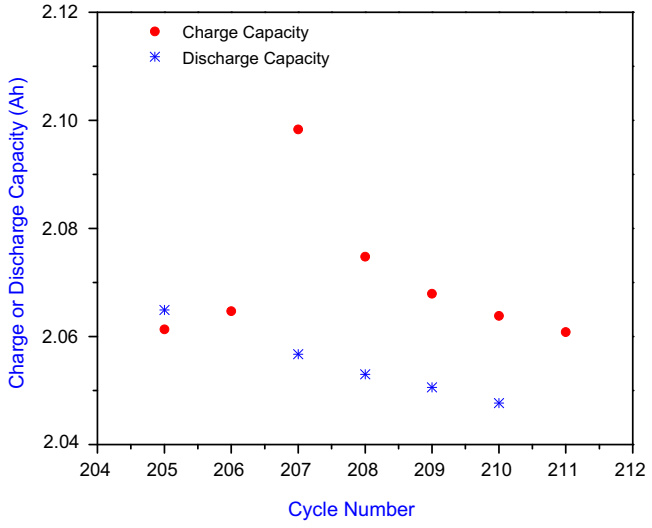

Fig. 5. Charge (●) and discharge (✳) capacities measured between 205 and 211 cycles in a 23.5 °C T_{env} after 204 cycles of CC-only charging. The 205–211 cycles used the CC–CV protocol for charging. (For interpretation of the references to colour in this figure legend, the reader is referred to the web version of this article.)

the manufacturer's guarantee of 30% capacity fading (1.785-Ah discharge capacity) at the end of 299 cycles.

It is interesting to note that the capacity fading was normal even though the cell voltage, E_{cv} far exceeded the 4.2 V for every one of the 204 cycles. Fig. 6 shows the end of the charge E_{cv}, which was also the maximum cell voltage. Note that past 200 cycles, E_{cv} was close to 4.6 V. The cell impedance, Z_{cell} recorded at the 45th, 205th and 211th cycle are shown as an inset in Fig. 6. The Z_{cell} gradually increase over the 211 cycles, which is a normal behavior for any Li-ion cell subject to the CC–CV charging protocol [21,22].

After the end of the 211th cycle, when the cell had been discharged by 1.3-Ah, we stored it at that state at 23 °C for nearly 7 months. We then discharged it at 1.3-A rate to determine capacity fading during storage. The cell yielded 0.78-Ah, for a total of 2.08-Ah, the same amount it did before the 7-month storage period, demonstrating that the CC-only charging during the first 204 cycles did not induce capacity fading during storage.

Thus, the CC-only charging procedure does not appear to degrade the cell or change its properties any more than the CC–CV procedure does.

3.4. Managing the risk of gassing and thermal runaway during CC-only charging

One of the perceived risks of CC-only charging is the possibility that the anode and cathode potential might reach high enough values to enable reduction and oxidation of the organic solvents. Most of the reaction products of reduction and oxidation of the solvents are gaseous [17] and could be toxic when combined with a high internal temperature (T_{int} > 250 °C) [23]. Data in Ref. [20] show that for the reduction or oxidation to occur, the cell voltage must exceed 4.5 V. Similarly, the conventional perception is that for thermal runaway to start, T_{int} must be >100 °C [24,25]. Published literature has been ambiguous about which one comes first: thermal runaway or gassing. The data in Figs. 2–4 and the discussions in Section 3.1 demonstrate that the entropy change in the anode could generate sufficient thermal energy to cause gas generation and venting without raising T_{int} to 100 °C, or without thermal runaway.

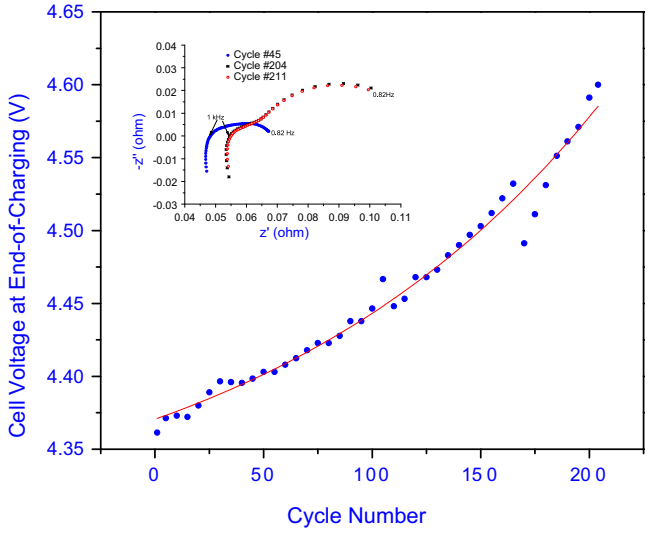

Fig. 6. The end of charge E_{cv} between 1 and 204 cycles CC-only charging. The graph only shows the E_{cv} data for every 5th cycle. The dotted line is an exponential fit with a correlation coefficient of 0.975. The inset shows the cell impedance measured at end of the 45th cycle (●), 204th cycle (✳) and 211th cycle (○); the measurements covered a range of 0.82 Hz to 800 Hz. Compare the impedance data with those in Fig. 1b.

Overcharging using the CC-only procedure at a rate between C/2 and 2C caused the cell to vent even though the cell voltage was<4.5 V and T_{anode} was <95 °C. In arriving at these conclusions, we speculate without direct evidence that the reason for the observed venting and gas evolution during overcharging was caused by entropy-initiated structural changes in the SEI layer: the entropy change disrupted the SEI layer that in turn initiated chemical reactions between the anode and the electrolyte. One important consequence of our finding is that monitoring T_{anode} during charging is far more reliable and useful than monitoring T_{surf} in preventing venting.

Overcharging continues to be one of the two major causes of venting and fires observed in Li-ion cells; the other major cause is internal shorts. Techniques aimed at minimizing the failures are described in a 2006 review article by Prem Kumar et al.. These same techniques have been further highlighted in two 2012 reviews published by two other groups [1,3]. A new technique for identifying emerging thermal runaway caused by 'latent defects' and internal short is being developed and validated by Kim et al. of the National Renewable Energy Laboratory (NREL) [26]. The BIT sensor described in this paper is a new addition to these emerging tools that help prevent overcharging and venting, enable fast charging, and help evaluate the thermodynamic properties (entropy, for instance) of the anode and cathode, in situ, in fully constructed Li-ion cells.

4. Conclusions

Entropy change (ΔS) in the anode plays a critical role during charging of Li-ion cells. During charging, the entropy-related thermal energy ($\Delta Q_{anode\ entropy} = T_{anode}\Delta S_{anode}$) dominates over Joule heating across the anode resistance ($I^2_{charge}\ R_{anode}t$), thus determines the rate of increase in anode temperature. During overcharging, $Q_{anode\ entropy}$ appears to be sufficiently large to disrupt the SEI layer allowing chemical interaction between the carbon anode and the solvents generating gaseous products leading to venting. The CC-only procedure for charging demonstrated that venting occurred before the cell voltage, E_{cv} raised above 4.5 V, before the solvents underwent electrochemical oxidation or reduction, and before the T_{anode} increased above 373 K; the >4.5 V and >373 K have been the limits quoted in the published literature to explain solvent decomposition and overcharge-induced venting [1,22,23].

More importantly, we now have a non-invasive technique to monitor T_{anode} online during charging [13–15]. Monitoring the rate of increase in T_{anode} provides two major gains: i.) Overcharging can be prevented during charging; and ii.) CC-only procedure charging can be used for charging, reducing the time of charging without the risk of overcharging. The maximum chargeable capacity is set by an apparent limit of $Q_{anode\ entropy} \rightarrow$ 224 J for the SDI 26F 18650 cell; this is equivalent to 2360-J mol^{-1} of lithium insertion into the carbon anode. At the 2360-J mol^{-1} limit, the anode temperature begins to rise sharply. If charging is continued beyond this limit, the cell would vent. The $Q_{anode\ entropy}$ limit is easily identified by measuring the anode temperature, T_{anode}: the rate of change of T_{anode} with charging time (dT_{anode}/dt) is sharp at the limit. The CC-only protocol, at the C/2 rate at 23.5 °C, if monitored and limited by the BIT sensor, does not degrade the cell any faster than the conventional CC–CV charging protocol.

Acknowledgements

The authors would like to thank Kim A. Cooper, Radiation Belt Storm Probes Project Manager at APL, for her support, Johns Hopkins University Applied Physics Laboratory (APL), the Independent

Research and Development programs by the National Security Space Business Area and the Research and Exploratory Development Department Business Area of the Applied Physics Laboratory (APL), the Johns Hopkins University for financial assistance. The authors would like to thank Carson Baisden, Michael Butler and Jeremy Walker of the APL and L. (Ram) Srinivasan of UCLA for valuable discussions. One of the authors (RS) wishes to thank Janney Publication Program of APL for financial support to prepare the manuscript.

References

[1] Q. Wang, P. Ping, X. Zhao, G. Chu, J. Sun, C. Chen, J. Power Sources 208 (2012) 210–224.
[2] C.-H. Doh, D.-H. Kim, H.-S. Kim, H.-M. Shin, Y.-D. Jeong, S.-I. Moon, B.-S. Jin, S.W. Eom, H.-S. Kima, K.-W. Kim, D.-H. Oh, A. Veluchamy, J. Power Sources 175 (2008) 881–885.
[3] L. Lu, X. Han, J. Li, J. Hua, M. Ouyang, J. Power Sources 226 (2013) 272–288.
[4] Shriram Santhanagopalan, Premanand Ramadass, John (Zhengming) Zhang, J. Power Sources 194 (2009) 550–557.
[5] C. Forgez, D.V. Do, G. Friedrich, M. Morcrette, C. Delacourt, J. Power Sources 195 (2010) 2961–2968.
[6] C.-Y. Lee, S.-J. Lee, M.-S. Tang, P.-C. Chen, Sensors 11 (2011) 9942–9950.
[7] V.V. Viswanathan, D. Choi, D. Wang, W. Xu, S. Towne, R.E. Williford, J.-G. Zhang, J. Liu, Z. Yang, J. Power Sources 195 (2010) 3720–3729.
[8] K. Smith, C.-Y. Wang, J. Power Sources 160 (2006) 662–673.
[9] S. Park, D. Jung, J. Power Sources 227 (2013) 191–198.
[10] Y. Reynier, R. Yazami, B. Fultz, J. Power Sources 119–121 (2003) 850–855.
[11] Y. Reynier, R. Yazami, B. Fultz, I. Barsukov, J. Power Sources 165 (2007) 552–558.
[12] R.E. Williford, V.V. Viswanathan, Ji-Guang Zhang, J. Power Sources 189 (2009) 101–107.
[13] Rengaswamy Srinivasan, J. Power Sources 198 (2012) 351–358.
[14] R. Srinivasan, B.G. Carkhuff, M.E. Butler, A.C. Baisden, Electrochim. Acta 56 (2011) 6198–6204.
[15] R. Srinivasan, B.G. Carkhuff, M.E. Butler, A.C. Baisden. Paper No. 8035-13, Security Sens. (25–29 April 2011).
[16] Y. Saito, K. Takano, A. Negishi, J. Power Sources 97–98 (2001) 693–696.
[17] W. Kong, H. Li, X. Huang, L. Chen, J. Power Sources 142 (2005) 285–291.
[18] K. Sato, M. Noguchi, A. Demachi, N. Oki, M. Endo, Science 264 (1994) 556–558.
[19] Gholam-Abbas Nazri, Gianfranco Pistiis (Eds.), Lithium Batteries: Science and Technology, Kluwer Academic Publishers, NY, 2004, p. 148.
[20] Gholam-Abbas Nazri, Gianfranco Pistiis (Eds.), Lithium Batteries: Science and Technology, Kluwer Academic Publishers, NY, 2004, p. 527.
[21] D.P. Abraham, E.M. Reynolds, E. Sammann, A.N. Jansen, D.W. Dees, Electrochim. Acta 51 (2005) 502–510.
[22] M. Broussely, Ph. Biensan, F. Bonhomme, Ph. Blanchard, S. Herreyre, K. Nechev, R.J. Staniewicz, J. Power Sources 146 (2005) 90–96.
[23] A. Hammami, N. Raymond, M. Armand, Nature 424 (2003) 635–636.
[24] Y.-B. He, F. Ning, Q.-H. Yang, Q.-S. Song, B. Li, F. Sub, H. Du, Z.-Y. Tang, F. Kang, J. Power Sources 196 (2011) 10322–10327.
[25] P.G. Balakrishnan, R. Ramesh, T. Prem Kumar, J. Power Sources 155 (2006) 401–414.
[26] G.-H. Kim, K. Smith, J. Ireland, A. Pesaran, J. Power Sources 210 (2012) 243–253.

Glossary

BIT: battery internal temperature
C: capacity of a cell in units of ampere-hour (Ah)
CC: constant current
CV: constant voltage
I_{charge}: charging current
$I^2_{charge}\ R_{anode}$: Joule heating in anode in units of Watt (W)
P_{resist}: power generated by Joule heating (W)
ΔQ: thermal energy generated by entropy change and Joule heating
$\Delta Q_{anode\ entropy}$: thermal energy generated by entropy change in the anode
R_{anode}: resistive impedance of the anode; it is a temperature-dependent parameter
$R_{cathode}$: resistive impedance of the cathode; it is a temperature-dependent parameter
R_{elec}: electrolyte resistance
R_{int}: internal resistance of a Li-ion cell ($R_{int} = R_{elec} + R_{anode} + R_{cathode}$)
SoC: state of charge
SEI: solid electrolyte interphase
ΔS: change in entropy
ΔS_{anode}: change in entropy of the anode
$\Delta S_{cathode}$: change in entropy of the cathode
t: charging time
T: temperature in K or °C
T_{anode}: temperature of the anode
$T_{cathode}$: temperature of the cathode
T_{env}: temperature surrounding the outer surface of the cell, typically the temperature of the environmental chamber
T_{int}: internal temperature of a Li-ion cell
T_{surf}: temperature at the outer surface of the cell measured by a K-type thermocouple mounted on the middle of the outer metal casing of the cell